Spectroscopic Detection of a Stellar-like Photosphere in an Accreting Protostar[1]

Thomas P. Greene
NASA's Ames Research Center, M.S. 245-6, Moffett Field, CA 94035-1000

Charles J. Lada
Harvard-Smithsonian Center for Astrophysics
60 Garden Street, Cambridge, MA 02138

ABSTRACT

We present high-resolution ($R \simeq 18,000$), high signal-to-noise 2 μm spectra of two luminous, X-ray flaring Class I protostars in the ρ Ophiuchi cloud acquired with the NIRSPEC spectrograph of the Keck II telescope. We present the first spectrum of a highly veiled, strongly accreting protostar which shows photospheric absorption features and demonstrates the stellar nature of its central core. We find the spectrum of the luminous ($L_{bol} = 10\ L_{\odot}$) protostellar source, YLW 15, to be stellar-like with numerous atomic and molecular absorption features, indicative of a K5 IV/V spectral type and a continuum veiling $r_k = 3.0$. Its derived stellar luminosity ($3\ L_{\odot}$) and stellar radius ($3.1\ R_{\odot}$) are consistent with those of a $0.5\ M_{\odot}$ pre-main-sequence star. However, 70% of its bolometric luminosity is due to mass accretion, whose rate we estimate to be $1.6 \times 10^{-6} M_{\odot}$ yr^{-1} onto the protostellar core. We determine that excess infrared emission produced by the circumstellar accretion disk, the inner infalling envelope, and accretion shocks at the surface of the stellar core of YLW 15 all contribute significantly to its near-IR continuum veiling. Its projected rotation velocity $v \sin i = 50$ km s^{-1} is comparable to those of flat-spectrum protostars but considerably higher than those of classical T Tauri stars in the ρ Oph cloud. The protostar may be magnetically coupled to its circumstellar disk at a radius of $2\ R_*$. It is also plausible that this protostar can shed over half its angular momentum and evolve into a more slowly rotating classical T Tauri star by remaining coupled to its circumstellar disk (at increasing radius) as its accretion rate drops by an order of magnitude during the rapid transition between the Class I and Class II phases of evolution.

The spectrum of WL 6 does not show any photospheric absorption features, and we estimate that its continuum veiling is $r_k \geq 4.6$. Its low bolometric luminosity ($2\ L_{\odot}$) and high veiling dictate that its central protostar is very low mass, M ~ 0.1 M$_{\odot}$.

Subject headings: stars:atmospheres, formation, and rotation — infrared: stars — techniques:spectroscopic

1. Introduction

The discovery of accreting protostars has been a triumph for understanding low-mass star formation. Infrared and sub-millimeter data have revealed that these objects are deeply embedded, cold, and luminous. The spectral energy distributions (SEDs) of such Class I protostars grad-

[1]Data presented herein were obtained at the W.M. Keck Observatory, which is operated as a scientific partnership among the California Institute of Technology, the University of California and the National Aeronautics and Space Administration. The Observatory was made possible by the generous financial support of the W.M. Keck Foundation.

ually rise from the near-IR, peak in the far-IR ($\lambda \sim 100\mu$m), and fall off in the sub-mm and mm wavelength regimes (**?**, e.g.,)]ALS87. Observations and models have indicated that protostars consist of three primary components: a massive infalling envelope, a circumstellar accretion disk, and an embryonic stellar core.

With a size of $\sim 10^4$ AU, the infalling envelope is the largest component of a protostellar object. It extends to within a few AU of the embryonic stellar core and absorbs and reprocesses all the visible (and UV) as well as much of the near-infrared radiation emitted by the central protostar. The infalling envelope contributes the bulk of the observed far-infrared to millimeter-wave luminosity and a significant portion of the detected near- and mid-infrared emission.

The circumstellar accretion disk can be as much as a few hundred AU in size and it contributes a significant portion of the observed mid- and near-infrared luminosity of the protostar. During the protostellar phase of evolution, the embryonic stellar core at its center grows primarily through accretion of material from the circumstellar disk, which itself acquires its mass directly from the infalling envelope.

The embryonic stellar core at the center of the protostar is thought to be a stellar-like object a few solar radii in extent (**?**, e.g.,)]SST80. It is the source of the bulk of the protostellar luminosity which is generated by both a strong accretion shock at the stellar surface and the radiation of internal stellar energy. This internal energy is provided by its self-gravity as well as the release of gravitational potential energy during the protostar's assembly from accreting and infalling material. The core's accretion-dominated luminosity is radiated primarily at UV and visual wavelengths, but most, if not all of this radiation is absorbed by dust in the infalling envelope which renders the central protostar invisible at these wavelengths. As a result, little is known about the nature of the embryonic stellar cores at the hearts of protostellar objects.

The observational technique of high-resolution near-IR spectroscopy has the potential to reveal the nature of these heavily embedded central objects. Indeed, we have recently been able to demonstrate the stellar nature of the central objects in flat-spectrum protostars and thus discern their spectral types, effective temperatures, rotation velocities, luminosity classes, and masses using this technique (Greene & Lada 1997, hereafter Paper I). These objects are in a later evolutionary state than Class I protostars; they are still surrounded by substantial circumstellar disks and envelopes but their accretion luminosities (and rates) have decreased below Class I levels. However, our previous high-resolution IR spectroscopic study of Class I young stellar objects (YSOs) did not reveal any spectral absorption features in these protostars (Greene & Lada 2000, hereafter Paper II). Luhman & Rieke (1999) did detect absorption features in the moderate-resolution near-IR spectrum of at least one Class I YSO (YLW 16A / IRS 44), but the moderate continuum veiling of that object ($r_k = 1$) suggests that it is intrinsically similar to a flat-spectrum YSO. Also, Kenyon et al. (1998) detected TiO absorptions in moderate-resolution optical spectra of three Class I YSOs in the Tau-Aur dark clouds. However, these are all low luminosity objects, $L_* \simeq L_{bol} \lesssim 0.5\ L_\odot$, indicating relatively low levels of accretion. Thus there is very little or no existing information concerning the nature and basic physical characteristics of the central stellar cores of protostars undergoing significant mass accretion.

Observational determination of the effective temperatures and radii (or surface gravities) of these deeply embedded central objects would provide critical constraints for theoretical protostellar models which predict the values of these parameters as a protostar evolves (Stahler, Shu, & Taam 1980). Empirical knowledge concerning the initial angular momentum of these objects as well as the evolution of angular momentum in the earliest phases of young stellar evolution is also highly desirable to test protostellar theory. Many classical T Tauri stars (CTTSs) embedded in the ρ Oph cloud and elsewhere are known to rotate slowly, $v \sin i < 20$ km s^{-1}. However, we have found that flat-spectrum protostars in this cloud have similar radii but rotate much more quickly, $v \sin i \simeq 40$ km s^{-1} (Paper I). Do heavily-accreting Class I protostars in Ophiuchus rotate as fast or faster? If so, how is stellar angular momentum reduced so quickly by the classical T Tauri pre-main-sequence (PMS) evolutionary phase?

We have undertaken a new, very sensitive near-IR spectroscopic study of Class I protostars with

the 10 m Keck II telescope in order to address these issues. The Keck observations are considerably more sensitive than our previous deep infrared spectral survey made with the 3-m NASA IRTF. In this paper we report our findings for two of these objects in the ρ Oph dark cloud, YLW 15 (IRS 43) and WL 6. These are 2 of the 3 ρ Oph Class I protostars detected in hard X-rays by the ASCA satellite, and both showed strong, variable, and flaring emission (Kamata et al. 1997). We describe our data acquisition and reduction in §2, analyze the spectra in §3, discuss the results in §4, and summarize our conclusions in §5.

2. Observations and Data Reduction

Near-IR spectra of the ρ Oph protostar YLW 15 were acquired on 2001 July 7 UT, and the protostar WL 6 was observed on 2000 May 30 UT. MK spectral standards were also observed 2000 May 29 – 30 UT. All data were acquired with the 10-m Keck II telescope on Mauna Kea, Hawaii, using the NIRSPEC facility multi-order cryogenic echelle spectrograph (McLean et al. 1998). Spectra were acquired with a $0\farcs58$ (4 pixel) wide slit, providing spectroscopic resolution $R \equiv \lambda/\delta\lambda =$ 18,000 (16.7 km s^{-1}). The plate scale was $0\farcs20$ pixel^{-1} along the $12''$ slit length, and the seeing was $0\farcs5$ – $0\farcs6$. The NIRSPEC gratings were oriented to allow both the 2.21 μm Na and the 2.30 μm CO band head regions to fall onto the instrument's 1024 × 1024 pixel InSb detector array, and its NIRSPEC-7 blocking filter was used. NIRSPEC was configured to acquire simultaneously multiple cross-dispersed echelle orders 31 – 36 (2.08 – 2.45 μm, non-continuous) in 2000 May and orders 32 – 38 (1.97 – 2.38 μm, non-continuous) on 2001 July 7. Each order had an observed spectral range $\Delta\lambda \simeq \lambda/67$ ($\Delta v \simeq 4450$ km s^{-1}).

The internal instrument slit rotator was used to maintain a fixed position angle on the sky when observing WL 6 and the MK standards on 2000 May 29 – 30. The slit was held physically stationary and thus allowed to rotate on the sky (as the non-equatorially-mounted telescope tracked) when observing on 2001 July 7 (YLW 15). Data were acquired in pairs of exposures of durations from less than 1 second (for giant MK standards) to up to 600 s (for the YSOs) each, with the telescope nodded $6''$ along the slit between frames so that object spectra were acquired in all exposures. WL 6 was observed for a total of 30.0 minutes, while YLW 15 was observed for 73.3 minutes. Early-type (B7 – A2) dwarfs were observed for telluric correction of the MK standard stellar spectra. HR 6054 (B7 IV) and HR 6070 (A0 V) were observed for telluric correction of the WL 6 and YLW 15 spectra, respectively. The telescope was automatically guided with frequent images from the NIRSPEC internal SCAM IR camera during all exposures of more than several seconds duration. Spectra of the internal NIRSPEC continuum lamp were taken for flat fields, and exposures of the its Ar, Ne, Kr, and Xe lamps were used for wavelength calibrations.

All data were reduced with IRAF. First, object and sky frames were differenced and then divided by flat fields. Next, bad pixels were fixed via interpolation, and spectra were extracted with the APALL task. Extracted spectra were typically 4 pixels ($0\farcs6$) wide along the slit (spatial) direction at their half-intensity points. Spectra were wavelength calibrated using low-order fits to lines in the arc lamp exposures, and spectra at each slit position of each object were co-added. Instrumental and atmospheric features were removed by dividing wavelength-calibrated object spectra by spectra of early-type stars observed at similar airmass at each slit position. Combined spectra were produced by summing the spectra of both slit positions for each object and then shifting the spectra in wavelength to correct for radial velocities. The standard spectra were shifted so that their lines matched laboratory wavelengths, while the YSO spectra were corrected for all Earth and solar system radial motions relative to the local standard of rest. The YSO spectra were not further corrected for the radial velocity of the ρ Oph cloud. Finally, YSO spectra were multiplied by an artificial spectrum of a T=10,000K black body in order to restore their true continuum slopes (although this was a small correction of under 10% per order).

3. Data Analysis and Results

3.1. Spectra

The spectra of several MK standard stars are shown in Figure 1. The three NIRSPEC orders with the most numerous absorption features are

displayed. These features are similar to ones seen by Wallace & Hinkle (1996) in stars of similar spectral type, although we present a finer grid of spectra in the K2V – M2V range. Spectra of these stars are dominated by strong features of Si (2.0923 μm), Mg (2.1066 μm), and Al (2.1099 μm) in the shortest wavelength order, with ratios Al/Mg and Al/Si being very sensitive to spectral type. Some of the strongest lines in the next order are Na (2.2062, 2.2090 μm), Sc (2.2058, 2.2071 μm), and Ti (primarily 2.2217 and 2.2240 μm). The Ti lines are very good indicators of spectral type in this range, growing stronger from earlier to later types. The 2.2069 μm Si line is also a good indicator of spectral type, weakening from early to later types. Therefore the ratio of Ti/Si is a particularly good spectral type diagnostic in this order. The strongest features in the longest wavelength order are Mg (2.2814 μm) and the CO $v = 0 - 2$ band head and rotation-vibration lines (2.2935 μm and long-wards). The Mg line becomes significantly weaker in later spectral types. All transitions identified above and hereafter (and in Fig. 1) occur in neutral species.

The two giant spectra (K3 III and M2 III) shown in Figure 1 have many of the same lines as the dwarfs, but there are significant differences. The Si and Mg lines in the shortest order do not appear to change monotonically with spectral type, but the lines in the next order are much more telling. The Sc (2.2058, 2.2071 μm) lines are very strong (absolutely and relative to Na) in the M2III giant, while the Ti lines are very strong in both giants. The Na lines (2.2062 and 2.2090 μm) are less broad in the giants because they are formed under conditions of lower pressure than in dwarfs. The Mg (2.2814 μm) line is also less broad in the giants and does not vary monotonically with spectral type. The 2.2935 μm CO band head and nearby rotation-vibration lines are very strong in the giants. Numerous other low-strength absorptions are seen in all three orders of the giant star spectra, indicating the presence of various molecules (**?**, see also)]WH96.

Three NIRSPEC spectral orders of the YSOs WL 6 and YLW 15 are shown in Figure 2. The WL 6 data have signal-to-noise of 100 – 170 at most wavelengths, and the YLW 15 data have signal-to-noise 240 – 300. Both objects have strong continua rising towards longer wavelengths. YLW 15

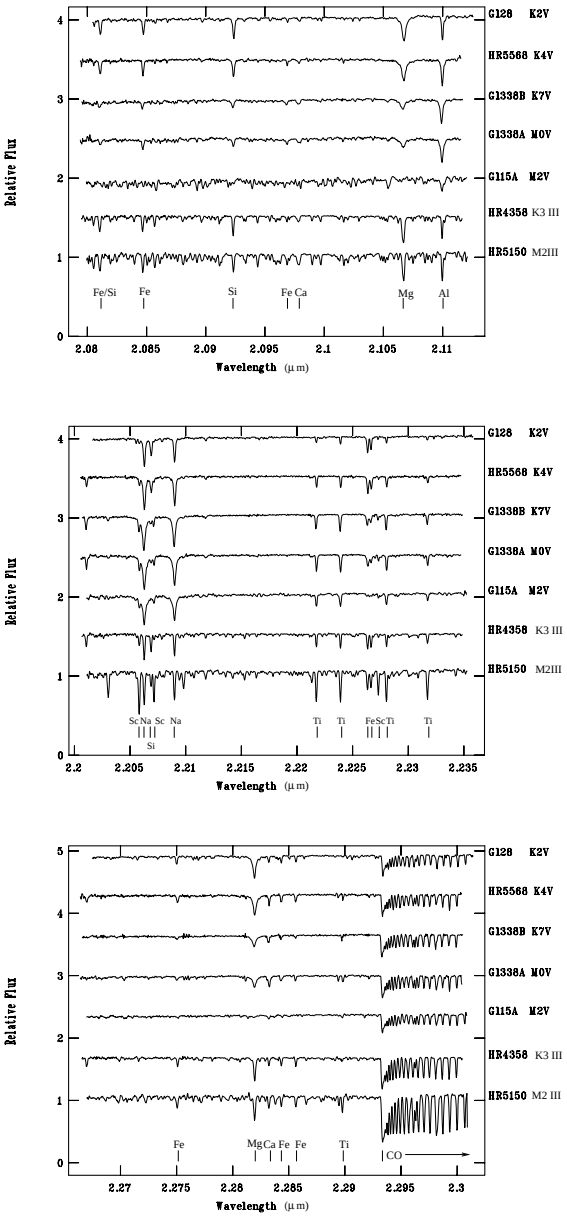

Fig. 1.— Spectra of MK standards. Three NIRSPEC orders are shown, and strong absorption features are identified in each order. Each of the three orders contain a number of lines whose ratios are useful for evaluating the spectral types of protostars independent of their veiling. Each spectrum has been normalized to a value of 1.0 and they are offset vertically by a constant in each order for separation.

has numerous absorption features which are weak and moderately broad, while any absorption features in the spectra of WL 6 are either weaker or non-existent. Both sources exhibit strong $v = 1 - 0$ S(0) H_2 emission at 2.2233 μm. Interestingly, the strength of this emission appears to be correlated with infrared excess and veiling in these objects. WL 6 has weaker (absent) absorption lines, a stronger red continuum, and stronger H_2 emission than YLW 15.

3.2. Veiling and Rotation Analysis

The spectra of YLW 15 and WL 6 are compared to those of the K4 dwarf HR 5568 in Figure 3. In this figure, the spectra of the YSOs are processed beyond that shown in Figure 2 in order to facilitate this comparison. First, their continuum slopes were removed by normalization. Next, the relative strengths of their absorption lines were magnified by subtracting off a constant continuum value of 0.75, 75% of the normalized continuum. This specific constant was chosen so that the absorption lines would have nearly the same equivalent widths in both YLW 15 and HR 5568. The spectrum of HR 5568 was modified by convolving it with a limb-darkened stellar rotation profile with velocity $v \sin i = 50$ km s^{-1}. This was required to match the velocity widths of its absorption features to those of YLW 15.

Figure 3 shows that the spectrum of YLW 15 is very similar to that of HR 5568. Nearly all absorption features have nearly identical *relative* strengths. Comparing relative line strengths is most useful because ratios (but not absolute equivalent widths) are insensitive to continuum veiling. For example, the ratios of their Mg (2.1066 μm) and Al (2.1099 μm) equivalent widths are very similar, as are the ratios of their lines in the Na and Sc region (2.2053 – 2.2096 μm). The lines in the Na and Sc region also have the same strengths relative to the Fe and Sc lines in the 2.2263 – 2.2273 μm region. However, the spectra of the two objects do not match exactly. The 2.2280 and 2.2317 μm lines of Ti are stronger relative to the 2.2053 – 2.2096 μm Na, Sc, and Si lines in YLW 15 than in HR 5568. Likewise, the 2.2814 μm Mg line is weaker relative to the CO band head (or the 2.2053 – 2.2096 μm Na, Sc, and Si lines) in YLW 15 than in HR 5568. Both of these differences suggest that YLW 15 is of slightly later spectral type than HR

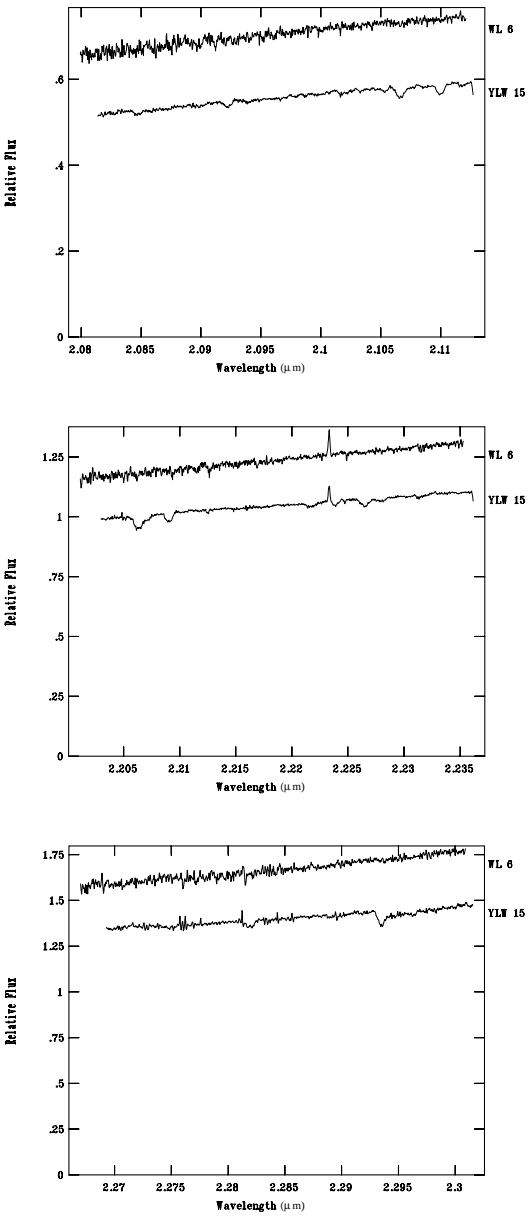

Fig. 2.— Spectra of Class I protostars YLW 15 and WL 6. The absorption lines are either weak (YLW 15) or undetected (WL 6) due to the large continuum veilings ($r_k \geq 3$) of these objects. Each spectrum has been normalized to a value of 1.0 (over all 3 orders), and WL 6 has been offset vertically by 0.2 for in each order for separation.

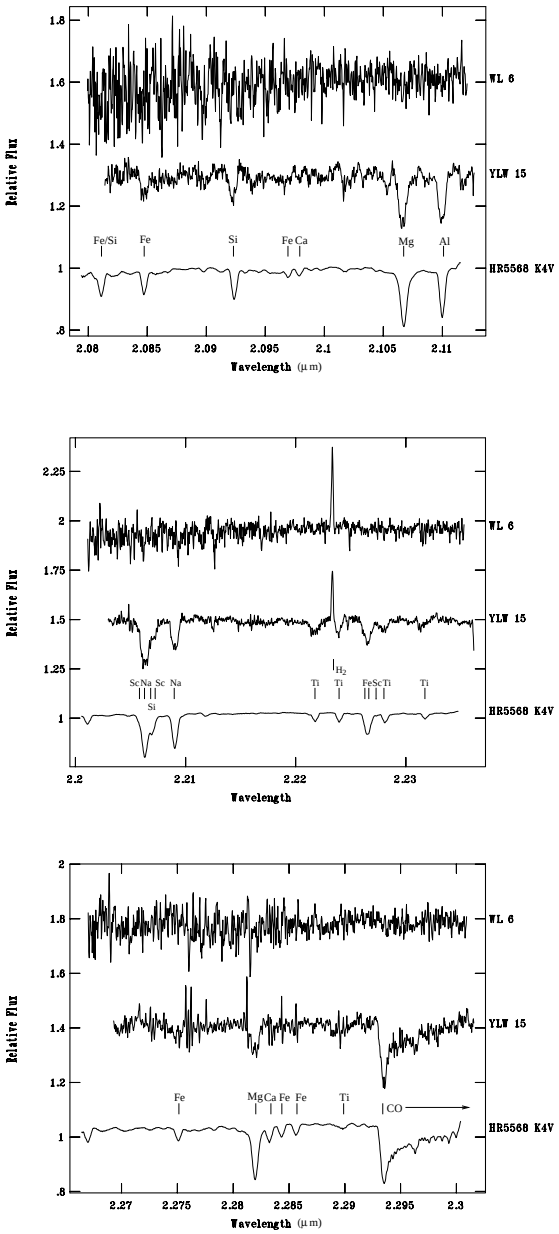

Fig. 3.— Spectra of YLW 15 and WL 6 compared to HR 5568 (K4 V). The spectra of the protostars have been normalized to remove their continuum slopes, and 75% of their continuum levels have been subtracted to remove the continuum veiling amount $r_k = 3$. Each spectrum has been normalized to a value of 1.0. The spectra are offset vertically by a constant in each order for separation.

5568. It is clear from Figure 1 that YLW 15 is not as late as Gl 338B (K7 V) and that its spectrum is much more dwarf-like than giant-like (see also the discussion of giant spectra in §3.1). We assign the spectral type K5 IV/V to YLW 15. Differentiating between luminosity class IV and V will probably require comparisons to synthetic model spectra given the rarity of well-classified luminosity class IV stars.

The continuum veiling of YLW 15 can be measured now that its spectral type has been determined. Continuum veiling at wavelength λ is defined as the value of continuum excess expressed as a fraction of the stellar photospheric flux, $r_\lambda = F_{\lambda,ex}/F_{\lambda *}$. We have estimated the K–band continuum veiling of YLW 15, r_k, by comparing the equivalent width of its K-band spectral features to those of MK standards. The above continuum veiling equation can be applied to K-band wavelengths and written in terms of the intrinsic (EW) and observed (EW') equivalent widths of spectral features there, $EW' = EW/(1 + \mathrm{r}_k)$.

We have evaluated r_k of YLW 15 by comparing the measured equivalent widths of its 2.2053 – 2.2096 μm Na, Sc, and Si lines (from its spectrum in Figure 2) to those of the K4 V star HR 5568 and the K7 V star Gl 338B. The measured equivalent widths of these features are 0.8, 2.8, and 3.5 Å for similarly-reduced spectra of YLW 15, HR 5568, and Gl 338B, respectively. The intrinsic equivalent widths of these features is expected to be approximately 3.2 Å for YLW 15, intermediate between HR 5568 and Gl 338B. Substituting these numbers into the above equation yields r_k = 3.0. We estimate that this value is accurate to about 25% given the uncertainties in the measured equivalent widths and the spectral type determination of YLW 15. This veiling implies that 75% of the K–band flux of YLW 15 arises from (circumstellar) continuum excess, and 25% of its flux arises from its K5 stellar photosphere. Therefore the stellar spectrum of this object can be approximated by subtracting 75% of the continuum level at K–band wavelengths. This – and normalization by its continuum – was done to produce the spectrum of YLW 15 shown in Fig. 3.

The derived veiling $r_k = 3.0$ of YLW 15 is considerably less than the $r_k \gtrsim 6$ which we estimated for this source in Paper II. There may be several reasons for this discrepancy. First, we have re-

examined the older, lower quality data of YLW 15 and have concluded that CO band head absorption may be present at low confidence in its spectrum (see Figure 2 of Paper II). The presence of such absorption would have lowered our estimate of the amount of veiling for this source. Second, the veiling in the protostar may have decreased during the 4 years which elapsed between our two observations. Luhman & Rieke (1999) found that ρ Oph sources can undergo large variations in veiling, and they also derive $r_k > 1$ from their 2 μm spectrum of YLW 15. Finally, in Paper II we assumed that YLW 15 was spectral type M0 when we estimated its veiling. Its actual spectral type is K5 (see above), which is expected to have intrinsically weaker CO absorptions (analyzed in paper II) than would a M0 star. This would have led to an overestimate of its veiling.

We have determined that the projected rotation velocity of the YLW 15 central protostar is v sin $i = 50 \pm 5$ km s^{-1}. This was measured by fitting its CO band head spectrum (Fig. 3c) to the spectrum of HR 5568 (K4 V) which had been convolved with stellar rotation profiles over a range of velocities. In order to confirm that this value was not influenced by any slight rotation of HR 5568 (whose rotation is unresolved in our spectra), we also fit the spectrum of YLW 15 with that of a slowly-rotating K giant star which had been convolved with stellar rotation profiles over a range of velocities. This also resulted in a projected rotation velocity of 50 km s^{-1}.

The spectra of WL 6 (Figs. 2 and 3) do not show any obvious absorption features, so only a lower limit to its veiling can be calculated. If the central protostar of WL 6 has the same spectral type and v sin i rotation velocity as YLW 15, then the signal-to-noise of its spectrum ($\sim$ 120 in the 2.2053 – 2.2096 μm region) dictates that WL 6 must have $r_k \geq 4.6$. This is consistent with the lower limit determined in Paper II, $r_k > 3.8 - 5.5$. This veiling analysis was based on maximum line depths (and not equivalent widths), so we expect the veiling of this object to be changed little if it is of later spectral type than YLW 15. Our analysis of dwarf standards indicates that although equivalent widths of the 2.2053 – 2.2096 μm features increase in later types (particularly in the M2 – M6 range), this is mostly caused by increasing intrinsic line widths (due to pressure broadening), with the peak line depths relatively unchanged. However, less veiling is required if WL 6 is rotating more rapidly than YLW 15, and more is required if it is rotating more slowly. Rotation can affect the measured line depths and veilings by about a factor of 2 over the range v sin $i = 0$ – 180 km s^{-1} (see Paper II).

4. Discussion

We have determined that the Class I YSOs WL 6 and YLW 15 have strong continuum veilings, and both have near-IR H_2 emission. Absorption lines in the spectrum of YLW 15 have allowed us to measure quantitatively its spectral type, r_k continuum veiling, and v sin i rotation velocity. We now examine and discuss the physical implications of these results given other information known about these YSOs.

4.1. YLW 15

The SED of YLW 15 rises steeply from the near- to the far-IR (2 – 60 μm) with a bolometric luminosity of approximately 10 $L_\odot$ (Wilking et al. 1989). Its 2 – 14 μm spectral index (slope of its SED) is 1.0 (Bontemps et al. 2001). André & Montmerle (1994) found that this source also has significant $\lambda = 1.3$ mm spatially-extended flux (100 mJy), which they interpreted as arising from its circumstellar envelope, confirming its Class I nature. Bontemps et al. (1996) found that YLW 15 has a compact molecular outflow which is seen nearly pole-on. The coexistence of molecular outflow and near-IR H_2 emission (Figs. 2 and 3) in this object is consistent with the correlation of these phenomena found by Greene & Lada (1996). GY 263 is a fainter near-IR source (**?**, $\delta K = 2.5$ mag;)]BKLT97 6″ ($\sim$ 900 AU projected distance) NW of YLW 15.

However, Girart, Rodríguez, & Curiel (2000) recently found that YLW 15 itself is binary in their $\lambda = 3.6$ cm VLA map. 2MASS (second incremental release) Point Source Catalog coordinates show that the 2 μm source is essentially coincident with VLA 2, the weaker, point-like radio source. VLA 1 is located approximately 0.″6 ($\sim$ 100 AU) to the NW and is spatially extended ($\sim$ 1″) SW – NE. Girart, Rodríguez, & Curiel (2000) interpret the VLA 1 emission to be thermal free-free, arising in a protostellar jet. HST / NICMOS near-IR im-

ages (F110W and F160W bands) show that the central source is single but embedded in extended nebulosity (Allen et al. 2002). Hereafter we assume that there is a central protostellar engine for YLW 15, and it is located at the VLA 2 / near-IR position. The VLA 1 source is likely to be emission from a jet produced by the central protostar and not a (proto-) stellar source itself.

One of the most intriguing aspects of YLW 15 is its X-ray emission. This was one of the very few Class I protostars which was detected by ROSAT (Casanova et al. 1995). Subsequent ROSAT HRI (Grosso et al. 1997), ASCA (Tsuboi et al. 2000), and Chandra (Imanishi, Koyama, & Tsuboi 2001) observations have all shown that its X-ray emission has frequent strong flares (**?**, $\sim 10^{33}$ erg s^{-1}; see)]GMFACG97,IKT01. The ASCA and Chandra observations have shown that its quiescent and flaring emissions consist of mostly hard X-rays. The ASCA observation captured 3 quasi-periodic flares with a $\sim$ 20 h period which spanned the exposure (Tsuboi et al. 2000), but the Chandra exposure captured only a single flare ($\sim$ 3 hr duration) in a 27.8 h exposure. Montmerle et al. (2000) have interpreted this flaring as arising from the interaction of the magnetic field of the rapidly rotating protostar (P $\simeq$ 20 h, near break up) and its slower rotating circumstellar disk.

Our near-IR spectrum of YLW 15 provides further information on the nature of this object. We have assigned it a spectral type of K5 IV/V (see §3.2), implying an effective temperature $T_{eff} \simeq$ 4300 K (Tokunaga 2000). Its near-IR spectrum (Fig. 3) shows no evidence for binarity; it shows no features which could arise in a companion of different spectral type. We now derive additional stellar and system parameters for this object.

4.1.1. Stellar Parameters

We used new near-simultaneous near-IR photometry (**?**, acquired 2001 July 8; see)]HBGR02 to estimate the extinction towards the central protostar of YLW 15. The observed CIT magnitudes of this object were $H = 12.53$ and $K = 9.35$ (undetected at J), and we de-reddened the $H - K$ color to determine that the extinction to the central protostar is $A_v \simeq 40$ mag. This value is intermediate between the lower limit ($A_v = 34$ mag), resulting from de-reddening to the maximum CTTS locus color $(H - K)_0 = 1.0$ mag (**?**, see)]MCH97, and the upper limit ($A_v = 47$ mag), resulting from de-reddening to the intrinsic stellar photospheric color $(H - K)_0 = 0.11$. YLW 15 cannot be accurately de-reddened to this stellar photospheric color because the de-reddened colors of Class I YSOs do not intersect stellar loci in near-IR color-color diagrams. This is due to the presence of both scattered light and infrared excess emission from the close-in circumstellar material contained in the surrounding accretion disk and infalling envelope (**?**, see)] LA92. Our adopted extinction ($A_v = 40$ mag) is consistent with the $A_v > 31$ mag value derived by Grosso et al. (1997) using a similar technique. Our extinction value, along with the measured near-IR excess $r_k = 3.0$, the IR extinction law, dwarf bolometric corrections, and a distance modulus of 6.0 yields an estimated *stellar* luminosity of 3.0 $L_\odot$. The 4300 K effective temperature of the protostar dictates that its stellar radius is 3.1 $R_\odot$. Although there are considerable uncertainties in extinction (and scattering), the derived protostellar properties are not greatly affected. Varying the A_v between its lower and upper limits changes the derived stellar luminosity by less than a factor of 2 and the derived stellar radius by less than 50%. The derived luminosity and radius are very similar to those predicted for a young PMS star of this effective temperature which is still accreting mass at a high rate (**?**, $\dot{M} \simeq 10^{-6} M_\odot$ yr^{-1}; see)]SFB99, TLB99. These and other modern PMS models indicate that the mass of YLW 15 is approximately 0.5 $M_\odot$, as determined from its effective temperature and stellar luminosity (D'Antona & Mazzitelli 1997; Siess, Forestini, & Bertout 1999; Siess, Dufour, & Forestini 2000). Taken with its derived radius, this dictates that the surface gravity of YLW 15 is Log $g \simeq 3.1$ (cgs units), within the range expected for a very young K5 PMS star.

4.1.2. Accretion

The derived stellar luminosity is about 30% of YLW 15's *bolometric* luminosity (Wilking et al. 1989), implying that 70% of the total luminosity of this protostar is due to mass accretion and not radiation of the protostar's internal energy. This accretion luminosity is likely to be composed of a component which arises in a circumstellar accretion disk as well as a component which is generated when accreting matter falls directly onto the

central protostar. If all matter accretes through a circumstellar disk with inner radius R_{in}, then the accretion luminosity arising in the disk as $GM\dot{M}_D/2R_{in}$ where $\dot{M}_D$ is the mass accretion rate through the disk. The accretion luminosity produced by matter falling from the disk edge R_{in} onto the star is $GM\dot{M}_*/R_* - GM\dot{M}_*/R_{in}$ where $\dot{M}_*$ is the mass accretion rate onto the star. We now assume that matter is transported from near the disk edge to the stellar surface in magnetospheric accretion columns (Koenigl 1991; Shu et al. 1994). In this scenario, matter accretes through the disk to a disk coupling radius R_x where it is then accreted onto the star along magnetic field lines (Shu et al. 1994). This point R_x is slightly exterior to R_{in}, and the total accretion luminosity of the system is

$$L_{acc} = \frac{GM_*\dot{M}_D}{2R_x} + \frac{GM_*\dot{M}_*}{R_*} - \frac{GM_*\dot{M}_*}{R_x}. \quad (1)$$

The typical inner hole radius of a CTTS circumstellar disk is $R_{in} \simeq 5R_*$ (Shu et al. 1994; Meyer, Calvet, & Hillenbrand 1997). Magnetospheric accretion models predict that the inner disk and coupling radii are closer to the central star when matter is accreting at higher rates, such as those typical for Class I protostars. DQ Her stars are also sometimes interpreted as exhibiting this behavior (**?**, e.g., see)]P94. We assume $\dot{M}_* = 0.7\dot{M}_D$ from Shu et al. (1994) and adopt their equation (2.6b) to express the magnetic coupling radius as

$$\frac{R_x}{R_*} = \alpha_x \left(\frac{B_*^4 R_*^5}{GM_*\dot{M}_D^2} \right)^{1/7} \quad (2)$$

where α_x is a constant on the order of 1 (Shu et al. 1994; Ostriker & Shu 1995).

We solved equations (1) and (2) simultaneously for mass accretion rates and R_x using the previously derived values of R_* (3.1 $R_\odot$), M_* (0.5 $M_\odot$), $\alpha_x = 0.92$ (Ostriker & Shu 1995), the above relation of mass accretion rates, and the assumption $B_* = 1000$ G. This results in a magnetic coupling radius $R_x = 2.1R_*$ and mass accretion rates $\dot{M}_D = 2.3{\times}10^{-6} M_\odot$ yr^{-1} and $\dot{M}_* = 1.6{\times}10^{-6} M_\odot$ yr^{-1}. This magnetic coupling radius is considerably uncertain (perhaps by 50%) because we have assumed a magnetic field strength and have not measured a value. The 2.2233 μm TI line is sensitive to magnetic (Zeeman) broadening, and indeed it has a larger equivalent width ($\sim$ 0.4 Å) in the stellar spectrum of YLW 15 than in either the K4 V standard HR 5568 (0.2 Å) or the K7 V standard Gl 338B (0.3 Å; see Figs. 1b and 3b). This suggests the presence of a significant (**?**, kG; e.g. see)]JVK99 magnetic field in YLW 15, but the magnitude of this field cannot be measured quantitatively from our spectrum due to its limited signal-to-noise and the presence of the flanking 2.2233 μm H_2 line (Fig. 3b).

The derived accretion rates are consistent with the accretion rates computed for other Class I YSOs in this cloud and are within a factor of 2 of the spherical accretion rate derived from the cloud's gas temperature (**?**, $\dot{M} = a^3/G$; see)]ALS87. The adopted 0.5 $M_\odot$ stellar mass of YLW 15 is also consistent with accretion at this rate (i.e. $\dot{M}_*$) over the mean Class I lifetime in the cloud (Greene et al. 1994; Luhman & Rieke 1999). The derived accretion rates and inner disk radius result in accretion luminosities of 2.75 $L_\odot$ arising in the disk and 4.25 $L_\odot$ arising at the stellar surface. Thus the stellar surface accretion luminosity is approximately 40% greater than the luminosity emanating from the T_{eff} = 4300 K protostellar photosphere. Calvet & Gullbring (1998) have shown that the region where an accretion column meets the surface of a T Tauri star has an effective temperature of approximately 8000 K. From this we calculate that the derived 4.25 $L_\odot$ stellar surface accretion luminosity arises from an area only 12% of the stellar surface.

4.1.3. Veiling

Here we investigate the possible sources of excess infrared continuum emission and their contributions to the overall veiling in the infrared spectrum of YLW 15. We consider three sources for the continuum veiling: the accretion luminosity generated at the surface of the protostar, the luminous accretion disk, and the inner infalling envelope. We calculate that the continuum from the hot accretion impact sites at the surface of the protostar will produce an effective veiling $r_k = 0.33$. Although a relatively small fraction of the total veiling, this is significantly greater than that predicted ($r_k < 0.05$) for accretion impact sites on typical class II T Tauri stars whose accretion rates

are substantially lower (Calvet & Gullbring 1998). Accretion models predict that the disk of YLW 15 ($L_{disk} = 2.75 L_{\odot}$) should contribute an IR veiling $r_k \sim 1.3$ (**?**, see Fig. 9 of)]GL96. The remainder of the object's observed veiling ($r_k \sim 1.4$ of $r_k = 3$ total) is likely to arise from grains in the circumstellar envelope of the protostar which are warmed by the photons produced by the stellar photosphere and at the hot sites of mass accretion. This implies that the envelope contains a significant amount of dust within ~ 0.3 AU of the central star (**?**, see also)]GL96, CHS97.

We note that the envelope veiling is low enough so that any absorption lines originating in the circumstellar disk should have been seen in the spectrum of YLW 15. However, the (stellar) dwarf-like natures of the YLW 15 absorption features imply that they are not formed in a circumstellar disk, which would show evidence of much lower surface gravity (see Paper I for a discussion and examples of FU Ori disk features). We calculate that the dust grain destruction distance (where $T \lesssim 1800$ K) for YLW 15 is approximately 10 R_* from considering both its protostellar photospheric and stellar accretion luminosities. This implies that the disk is completely gaseous and dust-free between $R_{in} = 2R_*$ and 10 R_*. The fact that we do not observe absorption lines arising in this disk region strongly implies that the gas in this region does not have a sufficient vertical temperature gradient to form strong spectral lines.

4.1.4. Rotation

The $v \sin i = 50$ km s^{-1} projected rotation velocity of YLW 15 is considerably greater than typical for many classical T Tauri stars, about equal to that found for flat-spectrum protostars in the ρ Oph cloud (see Paper I), and considerably less than the equatorial rotation velocity deduced for this object from its X-ray emission. If the 20 h X-ray flare period observed by Montmerle et al. (2000) was caused by rotation as they postulated, then assuming a 3.1 $R_{\odot}$ protostellar radius would imply an equatorial rotation velocity of approximately 180 km s^{-1}, approximately break up. If YLW 15 is rotating this fast, then its rotation axis must be only 16° from our line of sight. This is consistent with its molecular outflow being oriented nearly pole-on (Bontemps et al. 1996) if its outflow axis is aligned with its rotation axis. However, subsequent Chandra X-ray observations of YLW 15 do not support the interpretation that it is rotating with a 20 h period. These observations did not confirm flaring with a 20 h period; only one flare was detected in a 10^5 s (27.8 h) observation (Imanishi, Koyama, & Tsuboi 2001). This weakens the possibility that the ASCA X-Ray flare period is physically related to the protostellar rotation rate. The inclination – and hence the equatorial rotation velocity – of YLW 15 is not well constrained. In order to make quantitative comparisons, we assume that the rotation axis of YLW 15 is inclined 57° from our line of sight, the most likely inclination angle for a random distribution. This implies that its equatorial rotation velocity is approximately 60 km s^{-1}, but this is highly uncertain: our newly-determined parameters and previous data do not constrain this velocity well within the range $v_{rot} = 50$ – 180 km s^{-1}.

We estimate that the Keplerian co-rotation radius of the YLW 15 circumstellar disk is 2.0 R_* (for $v_{rot} = 60$ km s^{-1}), nearly equal to the $R = 2.1 R_*$ magnetic coupling radius. The co-rotation radius varies over the range of 2.3 – 1.0 R_* for the range of equatorial rotation velocities $v_{rot} = 50$ – 170 km s^{-1}. Due to its large uncertainty (see §4.1.2), we cannot determine whether the magnetic coupling radius is significantly different from the co-rotation radius over a large range of inclination angles. However, it appears that inclination angles $i \sim 65°$ (similar to our 57° assumption) are most compatible with the Shu et al. (1994) requirement that the co-rotation and magnetic coupling radii be essentially equal (provided that we have adopted the correct value of B_*).

If the central protostar and the disk are sufficiently magnetically coupled in this region, then the disk may be regulating the angular momentum (and rotation velocity) of the star (**?**, e.g.,)]K91,Eetal93,SNOWRL94. Although the observational evidence of such coupling in CTTSs has been recently challenged (**?**, e.g., see)]SMMV99,SMVMH01, the similarity of the co-rotation and coupling radii of YLW 15 are consistent with stellar spin-down and magnetic star–disk coupling. Indeed, we calculate that the magnetic braking time scale, $\tau \gtrsim |\dot{J}_*/(dJ/dt)|$ (**?**, F. Shu priv. communication; eq. 6 of)]H02, is only $\gtrsim 14{,}000$ yr for YLW 15. This is significantly

shorter than the $\sim 10^5$ yr age of Class I protostars, so YLW 15 is likely to have had more than enough time to couple magnetically to its disk.

Class II YSOs and CTTSs in the ρ Oph cloud (**?**, and CTTSs in Taurus; see)]Eetal93 are observed to rotate considerably more slowly (v sin $i \simeq 12$ km s^{-1}; see Paper I), so if YLW 15 is to evolve into a typical Ophiuchi CTTS it will likely lose about 75% of its angular momentum. This can result via disk braking if the protostar remains coupled or recouples to its disk as its mass accretion rate drops. If the mass accretion rate of YLW 15 suddenly dropped to $10^{-7} M_\odot$ yr^{-1}, then it would re-couple to its disk in only about 150,000 yr (**?**, i.e. eq. 6 of)]H02. This coupling would occur at a radius $R \simeq 4.5 R_*$ with co-rotation speed v sin $i \simeq 15$ km s^{-1} (for $i = 57°$), very similar to the mean rotation velocity observed for ρ Oph Class II YSOs. We note that this 150,000 year coupling time is much shorter than the mean age of ρ Oph Class II YSOs (5 – 10 $\times 10^5$ yr), so this can explain why Class II YSOs are observed to rotate more slowly than Class I and flat-spectrum ones. However, more sophisticated modeling is required to ascertain the exact nature of this spin-down behavior.

4.2. WL 6

Bontemps et al. (2001) found that WL 6 has a spectral index of 0.6 (over $\lambda = 2$ – 14 μm), less than that of YLW 15. Wilking et al. (1989) also found that the WL 6 spectral index is less than YLW 15, but their absolute values and the spanned wavelength range are different. WL 6 has a bolometric luminosity of approximately 2 $L_\odot$ (Wilking et al. 1989; Bontemps et al. 2001). Neither André & Montmerle (1994) or Motte, Andre, & Neri (1998) detected WL 6 at $\lambda = 1.3$ mm (peak $F_\nu < 20$ mJy in 11″ diameter), but both investigations regarded it as an embedded protostar due to its large spectral index. This source is not known to drive a molecular outflow (Bontemps et al. 1996), but it does have near-IR H_2 emission (Figs. 2 and 3). WL 6 source has no known companions, and it also appeared single at $\lambda = 2$ μm in the NIRSPEC camera images.

Kamata et al. (1997) found that WL 6 had a hard X-ray spectrum and its flux varied sinusoidally with a 23 h period, which they attributed to protostellar rotation. Montmerle et al. (2000) also modeled this variation as being due to rotation, but with a slower period (3.3 d). Imanishi, Koyama, & Tsuboi (2001) did not detect this sinusoidal variation, but they did detect two weak flares during their 10^5 s Chandra exposure. Taken with the results of YLW 15, we interpret these differences to indicate that the X-ray variability of WL 6 is not directly related to its protostellar rotation period. However, this cannot be confirmed until the rotation signature of a photospheric feature (such as 2.29 μm CO absorption) is observed in this object.

We have used the bolometric luminosity of WL 6 and the accreting PMS models of Siess, Forestini, & Bertout (1999) to bound the stellar parameters of this object. The stellar luminosity of WL 6 must be less than or equal to its bolometric luminosity, 2 $L_\odot$. The Siess, Forestini, & Bertout (1999) models predict that such a PMS star at a very young age ($\sim 10^5$ yr) must have mass $M_* \lesssim 0.3 M_\odot$ and $T_{eff} \lesssim 4000$ K (their Case B). The high veiling of WL 6 (see §3.2) implies that its stellar luminosity is considerably lower than 2 $L_\odot$. We now assume that WL 6 has approximately the same ratio of stellar to bolometric luminosity of YLW 15 since the r_k of WL 6 is somewhat larger and its T_{eff} is somewhat lower than YLW 15, with these effects tending to cancel each other. This implies that the stellar luminosity of WL 6 is $L_* \simeq 0.6 L_\odot$, with corresponding $M_* \sim 0.1 M_\odot$ and $T_{eff} \lesssim 3160$ K. This temperature is consistent with that of a M3 – M4 PMS star. Our previous models show that it is possible to produce significant veiling from only a circumstellar accretion disk for a PMS star of this mass (**?**, see Fig. 9 of)]GL96. However, it is also plausible and possible that matter may also accrete directly from the disk to the star, and some veiling could also be produced by its circumstellar envelope (all as in YLW 15). These limits on the mass, effective temperature, and luminosity of WL 6 imply that its mass accretion rate is on the order of $10^{-6} M_\odot$ yr^{-1}, from the relation $L_{acc} = L_{bol} - L_* = G M_* \dot{M} / R_*$. This rate is consistent with the typical $\sim 10^5$ yr Class I lifetime and the $\sim 0.1 M_\odot$ mass of WL 6.

5. Summary and Conclusions

We have presented the first spectrum of a highly veiled, strongly accreting Class I protostar (YLW

15 / IRS 43) which shows late-type photospheric absorption features. This spectrum has allowed us to diagnose a plethora of details about the stellar, accretion, and rotation properties of this protostar and its circumstellar environment. The spectrum of another Class I protostar, WL 6, did not show any photospheric absorption features. Both of these objects are known to have strong and variable hard X-ray emission. Our analysis of these spectra results in the following conclusions:

1. We have detected numerous late-type absorption features in the photosphere of YLW 15. These features include Si (2.0923 μm and 2.2069 μm), Mg (2.1066 μm), Al (2.1099 μm), Na (2.2062, 2.2090 μm), Sc (2.2058, 2.2071 μm), Ti (primarily 2.2217 and 2.2240 μm), and Mg (2.2814 μm) lines as well as the CO $v = 0-2$ band. All of these features are consistent with a single K5 spectral type (T_{eff} = 4300 K) with dwarf-like surface gravity (luminosity class IV/V).

2. YLW 15 has a low-mass central protostar ($M \simeq 0.5 M_{\odot}$) with effective temperature, surface gravity, and *stellar* luminosity similar to that of a T Tauri star despite its high bolometric luminosity ($L_{bol} \simeq 10\ L_{\odot}$). We find that the stellar luminosity of YLW 15 is 3 $L_{\odot}$ and its accretion luminosity is 7 $L_{\odot}$. Assuming the magnetic accretion model of Shu et al. (1994), we derive the disk mass accretion rate of YLW 15 to be $\dot{M}_D = 2.3 \times 10^{-6} M_{\odot}$ yr^{-1} and its stellar mass accretion rate to be $\dot{M}_* = 1.6 \times 10^{-6} M_{\odot}$ yr^{-1}. These rates are consistent with the mass accretion rate of the ambient cloud gas and the stellar mass of YLW 15 given the lifetimes of Class I protostars.

3. YLW 15 is highly veiled in the near-IR, $r_k \geq 3$. We explore the origin of this veiling and evaluate the contributions of the stellar surface accretion, circumstellar disk, and circumstellar envelope components. We estimate that the circumstellar disk and envelope contribute equally to the veiling each providing $\sim 45\%$ of the needed excess emission. We find a significant amount ($r_k \sim 0.33$) of veiling is provided by the accretion shocks at the stellar surface. Although this contribution is relatively small ($\sim 11\%$) compared to the total, it is significantly greater than that produced by similar processes in typical CTTSs. We determine that emission from the circumstellar envelope is inadequate to veil absorption features formed in the inner dust-free circumstellar disk. We conclude that there are no strong absorption lines formed in the warm inner disk of YLW 15.

4. The projected rotation velocity of YLW 15 is $v \sin i = 50$ km s^{-1}, much faster than that of a typical T Tauri star in the ρ Oph cloud. However, this rotation rate does not appear to be correlated with the X-ray flarings and variability observed in multi-epoch X-ray observations of this source. We do find that it is plausible that YLW 15 is magnetically coupled to its accretion disk at a radius of 2 R_* in the magnetic accretion model of Shu et al. (1994). This suggests – and we verify the plausibility – that stellar angular momentum decreases by over a factor of 2 in only $\sim 10^5$ yr between the protostellar and T Tauri evolutionary phases.

5. The near-IR spectrum of WL 6 does not show any obvious absorption features, and we estimate that the veiling of this YSO is $r_k > 4.6$. This high veiling and its low luminosity ($L_{bol} \simeq 2 L_{\odot}$) dictate that its central protostar is likely to have low stellar luminosity ($L_* \simeq 0.6 L_{\odot}$) and to be low mass ($M \sim 0.1 M_{\odot}$).

We thank Scott Kenyon and Robbins Bell for useful comments and discussions. The authors wish to recognize and acknowledge the very significant cultural role and reverence that the summit of Mauna Kea has always had within the indigenous Hawaiian community. We are most fortunate to have the opportunity to conduct observations from this mountain. We also thank the staff of the Keck Observatory for excellent support in the operation of the telescope and NIRSPEC. This research has made use of data products from the Two Micron All Sky Survey, which is a joint project of the University of Massachusetts and the Infrared Processing and Analysis Center/California Institute of Technology, funded by the National Aeronautics and Space Administration and the National Science Foundation. T. P. G. acknowledges grant support from the NASA Origins of Solar Systems Program, NASA RTOP 344-37-22-11. Finally, we thank NASA for providing and awarding time for these observations.

REFERENCES

Adams, F. C., Lada, C. J., & Shu, F. H. 1987, ApJ, 312, 788

Allen, L. E., Myers, P. C., Di Francesco, J., Math-

ieu, R., Chen, H., & Young, E. 2002, ApJ, 566, 993

André, P. & Montmerle, T. 1994, ApJ, 420, 837

Barsony, M., Kenyon, S. J., Lada, E. A., & Teuben, P. J. 1997, ApJS, 112, 109

Bontemps, S., Andre, P., Terebey, S., & Cabrit, S. 1996, A&A, 311, 858

Bontemps, S. et al. 2001, A&A, 372, 173

Calvet, N., Hartmann, L., & Strom, S. E. 1997, ApJ, 481, 912

Calvet, N. & Gullbring, E. 1998, ApJ, 509, 802

Casanova, S., Montmerle, T., Feigelson, E. D., & Andre, P. 1995, ApJ, 439, 752

D'Antona, F. & Mazzitelli, I. 1997, Memorie della Societa Astronomica Italiana, 68, 807

Edwards, S. et al. 1993, AJ, 106, 372

Girart, J., Rodríguez, L. F., & Curiel, S. 2000, ApJ, 544, L153

Greene, T. P. & Lada, C. J. 1996, AJ, 112, 2184

Greene, T. P., & Lada, C. J. 1997, AJ, 114, 2157 (Paper I)

Greene, T. P., & Lada, C. J. 2000, AJ, 120, 430 (Paper II)

Greene, T. P., Wilking, B. A., Andre, P., Young, E. T., & Lada, C. J. 1994, ApJ, 434, 614

Grosso, N., Montmerle, T., Feigelson, E. D., Andre, P., Casanova, S., & Gregorio-Hetem, J. 1997, Nature, 387, 56

Haisch, K. E. Jr., Barsony, M., Greene, T. P., & Ressler, M. E., preprint

Hartmann, L. 2002, ApJ, 566, L29

Imanishi, K., Koyama, K., & Tsuboi, Y. 2001, ApJ, 557, 747

Johns-Krull, C. M., Valenti, J. A., & Koresko, C. 1999, ApJ, 516, 900

Kamata, Y., Koyama, K., Tsuboi, Y., & Yamauchi, S. 1997, PASJ, 49, 461

Kenyon, S. J., Brown, D. I., Tout, C. A., & Berlind, P. 1998, AJ, 115, 2491

Koenigl, A. 1991, ApJ, 370, L39.

Lada, C. J. & Adams, F. C. 1992, ApJ, 393, 278

Luhman, K. L. & Rieke, G. H. 1999, ApJ, 525, 440

McLean, I. S. et al. 1998, Proc. SPIE, 3354, 566

Meyer, M. R., Calvet, N., & Hillenbrand, L. A. 1997, AJ, 114, 288

Montmerle, T., Grosso, N., Tsuboi, Y., & Koyama, K. 2000, ApJ, 532, 261

Motte, F., Andre, P., & Neri, R. 1998, A&A, 336, 150

Ostriker, E. C. & Shu, F. H. 1995, ApJ, 447, 813

Patterson, J. 1994, PASP, 106, 209

Shu, F., Najita, J., Ostriker, E., Wilkin, F., Ruden, S., & Lizano, S. 1994, ApJ, 429, 781

Siess, L., Dufour, E., & Forestini, M. 2000, A&A, 358, 593.

Siess, L., Forestini, M., & Bertout, C. 1999, A&A, 342, 480

Stahler, S. W., Shu, F. H., & Taam, R. E. 1980, ApJ, 242, 226

Stassun, K. G., Mathieu, R. D., Mazeh, T., & Vrba, F. J. 1999, AJ, 117, 2941

Stassun, K. G., Mathieu, R. D., Vrba, F. J., Mazeh, T., & Henden, A. 2001, AJ, 121, 1003

Tokunaga, A. T. 2000, in *Allen's Astrophysical Quantities Fourth Edition*, ed. A. N. Cox (New York: Springer), 143

Tout, C. A., Livio, M., & Bonnell, I. A. 1999, MNRAS, 310, 360

Tsuboi, Y., Imanishi, K., Koyama, K., Grosso, N., & Montmerle, T. 2000, ApJ, 532, 1089

Wallace, L., & Hinkle, K. 1996, ApJS, 107, 312

Wilking, B. A., Lada, C. J., & Young, E. T. 1989, ApJ, 340, 823

AAS LaTeX macros v5.0.